TransFGU: A Top-down Approach to Fine-Grained Unsupervised Semantic Segmentation

Zhaoyuan Yin^{1,2}*, Pichao Wang²†, Fan Wang², Xianzhe Xu², Hanling Zhang³†, Hao Li², Rong Jin²

¹College of Computer Science and Electronic Engineering, Hunan University

²Alibaba Group

³School of Design, Hunan University

{zyyin, jt_hlzhang}@hnu.edu.cn

{pichao.wang, fan.w, xianzhe.xxz, lihao.lh, jinrong.jr}@alibaba-inc.com

Abstract

Unsupervised semantic segmentation aims to obtain high-level semantic representation on low-level visual features without manual annotations. Most existing methods are bottom-up approaches that try to group pixels into regions based on their visual cues or certain predefined rules. As a result, it is difficult for these bottom-up approaches to generate fine-grained semantic segmentation when coming to complicated scenes with multiple objects and some objects sharing similar visual appearance. In contrast, we propose the first top-down unsupervised semantic segmentation framework for fine-grained segmentation in extremely complicated scenarios. Specifically, we first obtain rich high-level structured semantic concept information from large-scale vision data in a self-supervised learning manner, and use such information as a prior to discover potential semantic categories presented in target datasets. Secondly, the discovered high-level semantic categories are mapped to low-level pixel features by calculating the class activate map (CAM) with respect to certain discovered semantic representation. Lastly, the obtained CAMs serve as pseudo labels to train the segmentation module and produce final semantic segmentation. Experimental results on multiple semantic segmentation benchmarks show that our topdown unsupervised segmentation is robust to both objectcentric and scene-centric datasets under different semantic granularity levels, and outperforms all the current stateof-the-art bottom-up methods. Our code is available at https://github.com/damo-cv/TransFGU.

1. Introduction

Given pictures of this world, can a semantic concept be deduced by certain prior rules, or can it be induced from the massive amount of observations? The answer to this

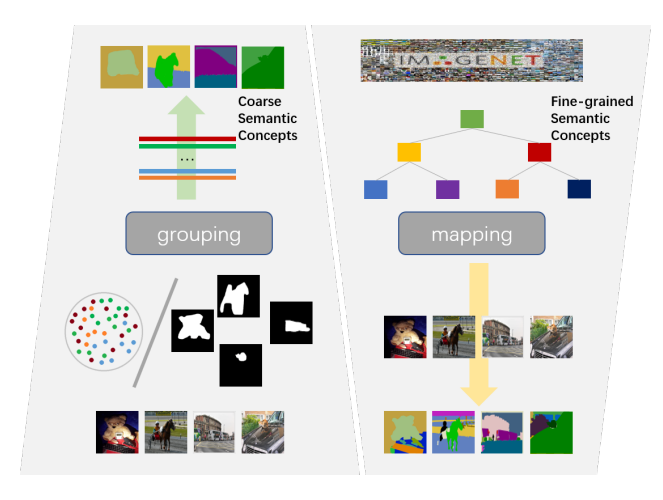


Figure 1. Bottom-up (left) *vs*. Top-down (right) frameworks. Currently bottom-up manners group feature under the guide of certain prior knowledge to form the semantic concepts (usually coarse), while our top-down manner maps the fine-grained structural semantic concepts obtained from ImageNet to pixel-level features and generate fine-grained segmentation.

question leads to different ways to obtain the semantic concept, and therefore brings different paradigms to the task of unsupervised semantic segmentation, which aims to obtain the pixel-wise classification as the semantic concept without any manual-annotated labels.

One way to tackle unsupervised image segmentation is to group low-level pixels into some semantic groups under the guidance of certain prior knowledge, *i.e.* the bottom-up manner [10, 16, 20, 21, 23, 28, 33], as shown in Figure 1. Those methods often assume pixels in the same semantic object share similar representation in the high-level semantic space. However, there is a large gap between low-level pixel and high-level semantic embeddings. Two semantically different objects may be mostly similar in low-level feature space, while the key to distinguish them lies in some small areas reflecting the uniqueness of a semantic category.

^{*}Work done during an internship at Alibaba Group.

[†]Corresponding author, project lead.

[‡]Corresponding author.

Accurate perception of this slight difference is the key to generate fine-grained segmentation, which is very hard to obtain by pixel-level deduction. In contrast, an object that has large intra-class variance on appearance may lead to dissimilar pixel-level features in different parts, which hinder the bottom-up methods from grouping these dissimilar features as an integrated object, due to the lack of high-level conceptual understanding of the whole object.

To alleviate these problems, this work proposes a topdown approach to unsupervised semantic segmentation, as shown in Figure 2. Instead of deducing high-level semantic concepts from low-level visual features, we start from the high-level fine-grained semantic knowledge induced from ImageNet. We benefit from the self-supervised learning method DINO [4] to gain the initial segmentation property of self-attention maps. The semantic representation obtained from DINO is more robust to the object appearance variations. Then we leverage the obtained prior to discover all the potential semantic categories presented in the target dataset, and group them into the desired number of semantic clusters according to their semantic similarity. It makes our method flexible to semantic concepts at different granularity level. We then project the high-level semantic information to low-level pixel feature space by Grad-CAM [31,39], to generate fine-grained active maps for various semantic classes. The obtained active maps serve as pseudo labels for segmentation model training. A bootstrapping mechanism is employed to iteratively refine the quality of pseudo labels and gradually improve the final segmentation performance. The proposed method, named as TransFGU, builds a bridge from high-level semantic representation induced by SSL to low-level pixel space, resulting in fine-grained segmentation in both object-centric and scene-centric images without any human annotations.

Through experiments on four public benchmarks, *i.e.* MS-COCO [26], PascalVOC [13], Cityscapes [11], and LIP [14], we show that our method can handle the cases of both foreground-only segmentation and foreground/background segmentation. Moreover, our method can control the semantic granularity level of segmentation by adjusting hyper-parameters, which overcome the limitations of previous methods that they can only produce coarse-level segmentation results. Our method achieves state-of-the-art results on all the benchmarks, surpassing current bottom-up methods with a large margin.

In summary, our contributions are as follows: (i) We propose the first top-down framework for unsupervised semantic segmentation, which directly exploits the semantic information induced from ImageNet to tackle the finegrained segmentation in an annotation-free way. (ii) We design an effective mechanism that successfully transfers the high-level semantic features obtained from SSL into low-level pixel-wise features to produce high-quality fine-

grained segmentation results. (iii) Experiments show that our proposed method achieves state-of-the-art on a variety of semantic segmentation benchmarks including MS-COCO, Pascal-VOC, Cityscapes, and LIP.

2. Related Work

2.1. Self-supervised Representation Learning

Self-supervised representation learning has rapidly gained attention for its promising ability to represent the feature of semantic concepts without additional labels. It is also beneficial to many downstream tasks including detection, segmentation, and tracking. The common paradigm of self-supervised representation learning is to minimize the feature distance between two views of the same objectcentric image [3, 4, 7–9, 15, 17, 24, 38]. It allows to learn semantic object concepts purely based on images from ImageNet without any annotations. The learned feature can perform well with KNN, which indicates the structuralsemantic concepts have been exploited. BYOL [15] shows that representation learning without a single label can be on par or even better than its supervised counterpart. DINO [4], a recent work based on the Transformer, shows that the selfsupervised learning method can learn a good representation of structured semantic category information, which has a nice property of focusing on the area of foreground objects. While most of them aim to learn the overall representation from the object-centric image, some others [25, 30, 34–37] tend to generate pixel-level dense features, which better benefit the tasks that require dense matching like segmentation or detection. However, all of these methods tend to learn the pixel-level correspondence on the category of objects that appear in different views of an image rather than learning the pixel-level semantic concept, so the learned representation embedding feature cannot convert to segmentation mask directly without additional manual labels.

2.2. Unsupervised Segmentation

Most of the current works proposed to tackle the unsupervised segmentation start from the observation of pixellevel features and grouping the pixels into different semantic groups with various priors rules that are independent of the training data. [21,23] group the similar pixel extracted from a randomly initialized CNN in both embedding and spatial space while keeping the diversity of embedding features. [16,20,28,29] maximize the mutual information between the pixel-level feature of two views from the same input image to distill the information shared across the image. PiCIE [10] disentangles features between different semantic objects by leveraging two simple rules, *i.e.* invariance to geometric and equivariance to photometric while transforming two different views of an image and its feature by two asymmetric augmentation processes. These rules often fail

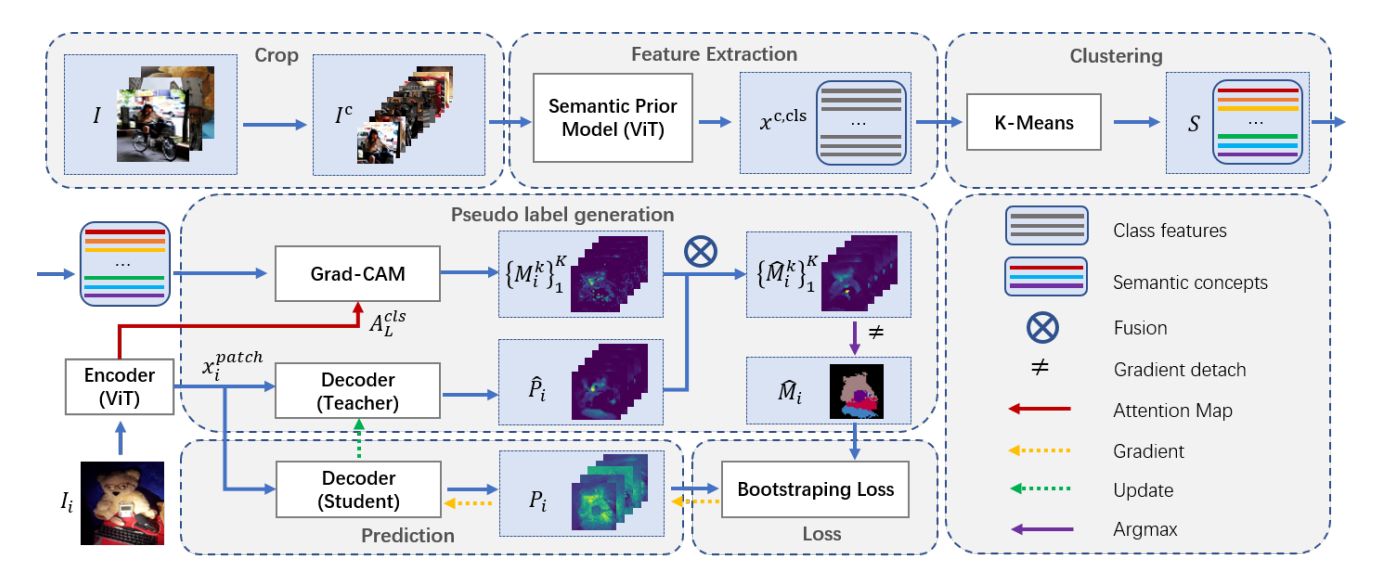


Figure 2. Our proposed top-down pipeline for unsupervised semantic segmentation. The training samples are first cropped and resized into square patches using sliding windows, and class features for each cropped patch are extracted by ViT pretrained on DINO. The obtained class features are clustered into semantic concept representations, which are mapped to pixel level to generate the pseudo labels. The quality of pseudo labels is further bootstrapped by the teacher network, based on which a student network is trained to refine the semantic knowledge. The teacher network is updated by the learned student network to produce better pseudo labels for the next round of training.

to tackle the case with complex scenes, where objects of different categories might share similar appearance and objects of the same category might have a large intra-class appearance variation. Unlike the bottom-up manner, our method is based on the top-down pipeline that obtains fine-grained semantic concepts prior information before performing the segmentation, which is crucial to tackling these two problems.

Besides the bottom-up methods, there are several works that use intermediate features as additional cues to guide the semantic feature grouping, including saliency map [1, 2, 6, 33], super-pixel [21, 28], and shape prior [19, 22]. MaskContrast [33] leverages two additional unsupervised saliency models to generate pseudo labels of the foreground object in each image and train the final segmentation model with a two-steps bootstrapping mechanism, and then cluster all the gathered foreground masks to form the semantic concept by contrast learning. However, these methods assume that objects in an image are salient enough, which is not always true in some complicated scene-based cases and could lead to low-quality segmentation.

3. Methods

Given a set of images $I = [I_1,...,I_N] \in [0,1]^{N\times 3\times H\times W}$ with total N samples, our goal is to generate a group of K segmentation probability maps for each image, denoted as $P = [P_1,...,P_N] \in [0,1]^{N\times K\times H\times W}$, where K indicates the predefined number of semantic categories to be segmented in I, and (H,W) are the height and width of image, respectively. To achieve this goal, an

encoder is first needed in the pipeline to extract pixel-level features for each image, and then a decoder is required to convert the pixel-level features into probability maps corresponding to each semantic category. In this section, we will first introduce some basics of the encoder and decoder, then describe the designed top-down pipeline, followed by a bootstrapping process which help further refine the results.

3.1. Revisiting ViT and Segmenter

Previous works on SSL have shown that ViT [12] models pretrained on ImageNet using methods like DINO [4] can provide surprisingly good properties for segmentation tasks due to its explicit semantic information learned during SSL. Thus, the pre-trained ViT is employed as ${\tt ENCODER}(\cdot)$ in our pipeline, for its capability of providing high-level semantic priors through the class token, as well as extracting pixel-level features in image patch tokens. Next, we will introduce some basic notations and terminologies about ViT for easier reference.

ViT is an attention based model with L layer attention blocks. Each attention block at the l-th layer produces an attention map $A_l \in [0,1]^{(1+hw)\times (1+hw)}$ that can be formulated as:

$$A_l = \text{Softmax}(\frac{Q_l \cdot K_l^{\text{T}}}{\sqrt{d'}}) \tag{1}$$

where $Q_l, K_l \in R^{(1+hw)\times d'}$ are the query and key, respectively, which are mapped and reshaped from the layer input x_l , and d' is the dimension of embedding feature in attention block.

As an $ENCODER(\cdot)$, the final outputs of ViT are denoted as class token x^{cls} and image patch tokens as x^{patch} . It is worth noting that, ViT pretrained with DINO is more irreplaceable for generating high-level semantic priors through class token, however, the model for generating pixel-level features can be substituted by other networks capable of extracting nice local features. Here we unify the two networks as the same ViT model for simplicity.

For the decoder which generates segmentation probability maps using the output of encoder, there are also lots of options while transformer-based methods are preferable due to their robustness to noises. Segmenter [32] is selected among them for its simplicity and straightforward interface to take x^{patch} as input.

Segmenter is a transformer-based segmentation model which consists of multiple cross-attention layers. It takes x^{patch} as input, and the output probability mask is:

$$Mask(x', C) = \frac{x'C^{T}}{\sqrt{d}}$$
 (2)

where x' and $C \in R^{K \times d}$ are the patch embedding and class embedding output by the final layer in the segmenter, respectively. $MASK(x',C) \in \mathbb{R}^{hw \times K}$ is the downsampled probability maps for K categories, and then it is upsampled to (H, W) to obtain the final mask P. This whole process is denoted as $DECODER(\cdot)$ in the following sections.

3.2. Top-down pipeline

An image might contain abundant and complex semantic concepts instead of a simple object, therefore, applying encoder on the whole image might not be sufficient to attend to all potential semantic priors. Instead, we propose to apply a sliding window cropping operation to each image. For every image I_i , n_c square patches are generated, each with side length $\beta \times \min(H, W)$ where β is a scaling factor taking a series of values. Patches from all images are put together to form a larger "patch image" set $I^c = [I_1^c, \dots, I_N^c]$ with I_i^c representing the patch set for image I_i . All patches are resized to $(\frac{\min(H,W)}{2}, \frac{\min(H,W)}{2})$ and treated as a whole image before feeding into the ViT encoder.

Class features and patch features are extracted from I^c , denoted as $x^{c,cls}=[x_1^{c,cls},\ldots,x_N^{c,cls}]$ and $x^{c,patch}=$ $[x_1^{c,patch},\ldots,x_N^{c,patch}]$, in which:

$$(x_i^{c,cls}, x_i^{c,patch}) = \text{Encoder}(I_i^c)$$
 (3)

here the ViT encoder is served as a semantic prior model, $x^{c,cls}$ can be regarded as containing all the potential semantic concepts that have appeared in I, $x^{c,patch}$ is discarded because of its weak semantic prior property. Assuming there are in total K pre-defined semantic categories, we can obtain a set of semantic feature $S = [S_1, \dots, S_K] \in \mathbb{R}^{N \times d}$ by applying K-means on $x^{c,cls}$ based on Euclidean distance.

K can be set as the number of classes, to generate segmentation results at different desired granularity levels.

Next, Grad-CAM [31] is employed to map these toplevel semantic features S to bottom pixel-level features. The semantic information mapped from $S_k \in S$ by Grad-CAM is aggregated at each pixel location to generate the response map, which can be treated as pseudo labels M = $[M_1,\ldots,M_N],\,M_i\in[0,K]^{H\times W}$. Furthermore, a decoder will be trained based on these pseudo labels.

To be more specific, inspired by [5], we first obtain the class token x_i^{cls} and patch token x_i^{patch} of the whole image I_i by ViT encoder:

$$(x_i^{cls}, x_i^{patch}) = \text{ENCODER}(I_i),$$
 (4)

then take attention map from cls token of the last attention block, and take the feature map while discarding the cls token itself. Denote $A_L^{cls} \in [0,1]^{h \times w}$ as the feature map, gradient is generated on A_L^{cls} w.r.t S_k by maximizing the cosine similarity between x_i^{cls} and each $S_k \in S$:

$$\min(1 - \frac{x_i^{cls} S_k^{\mathrm{T}}}{\sqrt{d}}). \tag{5}$$

We take the gradient value of all the patch locations on A_L^{cls} , and add it back to A_L^{cls} to generate K maps as pseudo labels:

$$\begin{split} M_i &= \underset{h \in H, w \in W}{\max} \left(M_i^1, \dots, M_i^K \right), \\ M_i^k &= \text{GRAD-CAM}(x_i^{cls}, S_k | A_L^{cls}) + A_L^{cls}. \end{split} \tag{6}$$

$$M_i^k = \text{GRAD-CAM}(x_i^{cls}, S_k | A_L^{cls}) + A_L^{cls}. \tag{7}$$

If only the foreground objects needs to be segmented in an image, we calculate the background probability M_i^{bg} based on all the foreground pseudo labels as follows:

$$M_i^{bg} = \text{ReLU}(T^{bg} - \max_{k \in [0,K]} M_i^k) \tag{8}$$

in which T^{bg} is a hyper-parameter that represents the max probability of background, and set to 0.1 in our experiments. M_i^{bg} is then concatenated with M_i . The decoder can be trained by standard cross-entropy loss with its output denoted as segmentation probability maps P:

$$\mathcal{L} = CE(P, M). \tag{9}$$

3.3. Bootstrapping

Training the decoder directly with the initial pseudo labels may lead to segmentation of low quality because the noise level in pseudo labels can be detrimental. For example, two categories with similar high-level semantic meaning may generate similar response maps on the same image, thus disturbing the ranking of K values on the same location of the pseudo labels and further misleading the learning process. Additionally, the boundary produced by the pseudo labels is not precise enough for certain semantic objects. As shown in Figure 6, a CAM may contain several scattered areas with low response values besides the high response area of the target object.

We tackle these problems by a bootstrapping mechanism. First, a teacher-student framework is introduced to refine the pseudo labels progressively. Second, we introduce a set of loss functions to force the model to learn discriminative abilities and prevent the model from over-fitting to the noise in the pseudo labels.

Teacher-Student Network. In our design, both teacher and student network have exactly the same architectures as DECODER(·). As shown in Figure 2, given an initial pseudo mask M generated by Grad-CAM, its bootstrapped version $\hat{M} = [\hat{M}_1, \dots, \hat{M}_N]$ can be obtained by aggregating M and the output of the teacher network prediction $\hat{P} = [\hat{P}_1,...,\hat{P}_N] \in [0,1]^{N \times K \times H \times W}$:

$$\hat{P}_i = \text{TEACHER}(x_i^{patch}), \tag{10}$$

$$\hat{M}_{i} = \underset{h \in H, w \in W}{\arg \max} (\hat{M}_{i}^{1}, \dots, \hat{M}_{i}^{K}), \qquad (11)$$

$$\hat{M}_{i}^{k} = 0.5 \cdot (M_{i}^{k} + \hat{P}_{i}^{k}), k \in [1, \dots, K]. \qquad (12)$$

$$\hat{M}_i^k = 0.5 \cdot (M_i^k + \hat{P}_i^k), k \in [1, \dots, K].$$
 (12)

With this bootstrapped pseudo labels, the student network is trained with a cross-entropy loss CE(P, M) with P as the output segmentation probability of student network, i.e. $P_i = \text{STUDENT}(x_i^{patch}).$

In the next round, the teacher network is updated with the parameter trained from the student network, so it can produce better prediction of \hat{P} , which further improves the bootstrapped pseudo labels \hat{M} . The student network in the next round is reset to the initial state and trained with the improved \hat{M} . Therefore, the quality of bootstrapped pseudo labels and the output of the student network can be improved progressively as the iteration goes on.

Bootstrapping Loss. A few additional loss functions are further proposed to provide better guidance for training the decoder based on the pseudo label masks.

First, we observe that even though categories with similar semantic meanings are difficult to differentiate thus might confuse the training process, categories with much different semantic meanings are actually easier to identify with high accuracy. Therefore, in addition to the crossentropy loss which aligns probability masks P and the "correct" pseudo labels \hat{M} , we also introduce a set of "wrong" pseudo labels \hat{M}' so that its cross-entropy loss with P should be maximized. Thus a peer loss [27] is defined as below:

$$\mathcal{L}_{peer} = CE(P, \hat{M}) - \alpha \cdot CE(P, \hat{M}'). \tag{13}$$

where α is a hyper-parameter, and \hat{M}' is the constructed negative labels by shuffling the K pseudo labels of M.

Second, it is observed that categories with similar semantic meanings usually generate similar response values at the same location of the pseudo label masks, making it hard to distinguish the correct category from the others and further slow down the training. An uncertainty loss is introduced to diminish such uncertainty. Specifically, this is achieved by maximizing the gap between the largest and the second largest value at each location of the output probability map P:

$$\mathcal{L}_{unc} = 1 - \frac{1}{hw} \sum_{h \in H} \sum_{w \in W} (p' - p'').$$
 (14)

in which p', p'' are the largest and second largest probability value among the K probabilities at location (h, w).

Third, it is beneficial to keep the representations diversified in the decoder model to learn more meaningful categories information. This is done by a diversity loss which maximizes the summation of all the pairwise distances between the class embeddings of K categories, i.e., minimizing their cosine similarities:

$$\mathcal{L}_{div} = 1 + \frac{1}{K^2} \sum_{i} \frac{C \cdot C^T}{\sqrt{d}}.$$
 (15)

where C is the class embedding in the decoder as in Eq. 2. The final loss is:

$$\mathcal{L} = \mathcal{L}_{peer} + \omega_1 \cdot \mathcal{L}_{div} + \omega_2 \cdot \mathcal{L}_{unc}. \tag{16}$$

in which ω_1, ω_2 are hyper-parameters to balance between different losses, and set to 1 and 0.3 in our experiments, respectively.

4. Experiments

4.1. Dataset and Evaluation Metrics

We conduct experiments on four semantic segmentation benchmarks including COCO-Stuff, Pascal-VOC, Cityscapes, and LIP, with different definitions of semantic concepts.

COCO-Stuff. COCO-Stuff is a challenging benchmark with scene-centric images, which contains 80 things categories and 91 stuff categories. The total number of training and validation samples is 117,266 and 5,000 images, respectively. Note that we conduct our experiments based on all the samples in COCO-Stuff, unlike previous works [10, 20] that use only the 'curated' data in which the stuff occupied at least 75% pixels of an image. We evaluate our method on three settings: 1) COCO-Stuff-27:all categories merged into 27 superclasses as [10], 2) COCO-Stuff-171: the original 171 things and stuff categories, and 3) COCO-80: only 80 things categories without background stuff.

Cityscapes. Cityscapes contain 5,000 images focusing on street scenes, in which 2,975 and 500 images are used for training and validation. All pixels are categorized into 34 classes. We follow [10] to merge 34 classes into 27 classes after filtering out the 'void' class.

Pascal-VOC. Pascal-VOC contains 1464 images for training and 1,449 for evaluation, with 20 classes as foreground objects to be segmented and the rest pixels as background.

LIP. LIP contains person images cropped from MS-COCO [26]. It has 30,462 training images and 10,000 validation images, with 19 semantic parts defined. The 19 categories are merged into 16 and 5 coarse categories to evaluate the ability of our method to handle the semantic concepts of different granularities. Please refer to supplementary materials for more details.

Evaluation Metric. Following the standard evaluation protocols for unsupervised segmentation used in [10, 20, 33], we use Hungarian matching algorithm to align indices between our prediction and the ground-truth label over all the images in the validation set. Two metrics are reported for comparison, *i.e.* Intersection over Union (mIoU) and Pixel Accuracy over all the semantic categories.

4.2. Implementation Details

Cropping and evaluation protocol The scaling factor β in sliding window cropping is set to 0.5, 0.4, 0.3, 0.2, and the step size of the sliding window is set to $\frac{1}{2} \times \beta \times \min(H, W)$.

Foreground prior is introduced in the cropping operation, which is defined as the binarized attention map \bar{A}_L^{cls} obtained from A_L^{cls} on the last attention block by setting the values greater than mean value of A_L^{cls} as 1 and the rest as 0. Cropped patches are separated into foreground patches and background patches. A patch is a foreground patch when it has more than 50% of pixels belonging to \bar{A}_L^{cls} , and a background patch when it contains more than 80% of pixels that belong to $(1-\bar{A}_L^{cls})$. K-Means is executed on these two groups of patches separately. If a patch is treated as a foreground patch, its probability on those background categories will have default value of 0, and a background patch is treated in a similar way. The separation of foreground and background patches helps generate more accurate semantic clusters and better pseudo labels.

Different cropping protocols are applied to the four datasets, due to their different properties and requirements. On Cityscapes, foreground prior is not involved as there is no definition of foreground/background. On LIP, the images are obtained as bounding boxes around each person without much background area, so we treat all the areas as foreground. On COCO-80, Pascal-VOC and LIP, Eq. (8) is used to generate background probability.

Trainning Setting We use *ViT-small* with patch size 8×8 pre-trained on ImageNet with DINO [4] as our encoder

backbone, and Segmenter [32] with random initial weights as the decoder. The encoder network is fixed through the whole training process to maintain the consistent semantic prior. Our model is trained on $4 \times \text{Tesla V}100\ 32\text{G}$ GPUs with Adam optimizer. As the pseudo label generation is time-consuming, we pre-compute all the initial pseudo labels and build a pseudo label bank which considerably accelerates the training.

Data Augmentation A set of data augmentations are utilized, such as color jittering, horizontal flipping, Gaussian blur, color dropping, and random resized crop following [4,15]. The cropped image is resized to $(\frac{H}{2}, \frac{W}{2})$ for the following training. We crop and resize the initial pre-computed pseudo label to $(\frac{h}{2}, \frac{w}{2})$ by RoI-Align operator [18].

4.3. Main Results

Baseline We compare our method with PiCIE [10], IIC [20] and MaskContrast [33], which can generate segmentation masks from images without further fine-tuning steps. Since IIC and PiCIE cannot distinguish foreground objects from the background, they can only be applied on COCO-Stuff and Cityscapes. MaskContrast is only able to deal with the foreground object without background area, so it is only be applied to COCO-80 and Pascal-VOC. None of these methods can actually work well on LIP which is essentially a task of fine-grained human parsing. Note that our method can be successfully adapted to all these datasets.

Quantitative evaluation. The comparison is shown in Table 1. Our method exceeds all the baseline methods on mIoU and pixel accuracy of all datasets. Our method has been adapted to different granularity levels in the same dataset, *e.g.* 27/171 categories on COCO-Stuff and 5/16/19 categories in LIP, to make a fair comparison with other methods which mainly work on coarser-level categories. Our method shows a larger margin of performance improvement for the settings with much finer-grained categories. Besides, it can also be adapted to only segment foreground objects, *i.e.* COCO-80, Pascal-VOC, and LIP, demonstrating its all-around flexibility.

Qualitative evaluation. Some qualitative comparisons on different benchmarks are shown in Figure 3,4,5. Our results can show richer semantic information in both scene/object-centric images on all datasets. We obtain much detailed segmentation on foreground (or Things) objects, especially in complicated scenarios.

CAM visualization. Figure 6 visualizes the class activate map generated by Grad-CAM. As one can see, the CAM can locate objects well in a very complex scene-based image and give a fine-grained activate map on the target location, which is crucial to our top-down segmentation pipeline.

Dataset	Method	mIoU	Acc
COCO-Stuff-27	IIC [20] PiCIE [10] PiCIE* [10] TransFGU	2.36 11.88 11.36 16.19	21.02 37.20 34.17 44.52
COCO-Stuff-171	IIC [20] PiCIE [10] PiCIE* [10] TransFGU	0.64 4.56 5.61 11.93	8.67 24.66 29.79 34.32
COCO-80	MaskContrast [33]	3.73	8.81
	TransFGU	12.69	64.31
Cityscapes	IIC [20]	6.35	47.88
	PiCIE [10]	12.31	65.50
	TransFGU	16.83	77.92
Pascal-VOC	MaskContrast [33]	35.00	79.84
	TransFGU	37.15	83.59
LIP-5	TransFGU	25.16	65.76
LIP-16	TransFGU	15.49	60.08
LIP-19	TransFGU	12.24	42.52

Table 1. Results on four benchmarks. * indicates the result is reproduced under the backbone of ResNet-50.

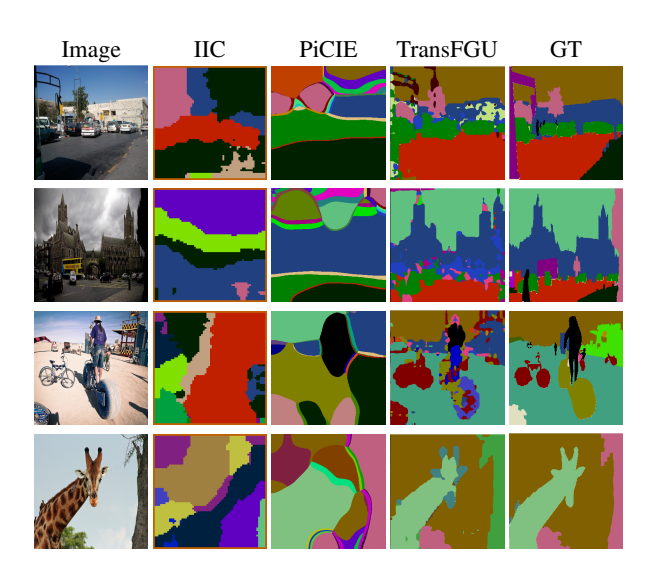


Figure 3. Qualitative comparison on COCO-Stuff-171.

4.4. Ablation Studies

The Bootstrapping Mechanism. Table 2 compares results on MS-COCO of directly using initial pseudo labels ("initial"), training the student network once on the initial pseudo labels without the bootstrapping ("trained"), and the proposed bootstrapping mechanism ("bootstrapped"). Student network trained once on the initial pseudo labels can achieve an improved mIoU over the original pseudo labels, indicating that it can effectively learn meaningful in-

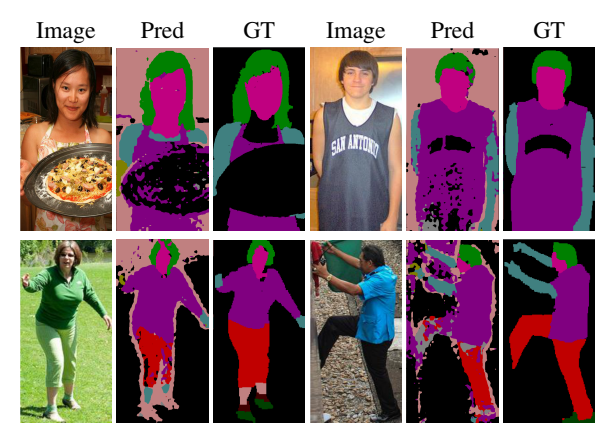


Figure 4. Qualitative results on LIP for 16 fine-grained semantic granularity.

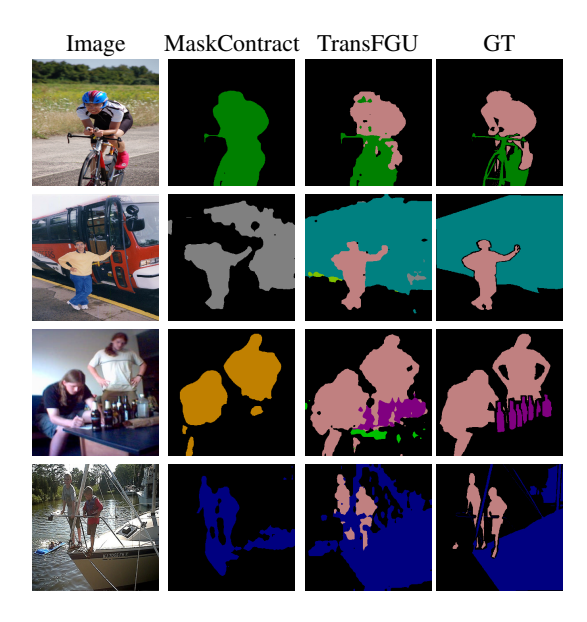


Figure 5. Qualitative results on Pascal VOC.

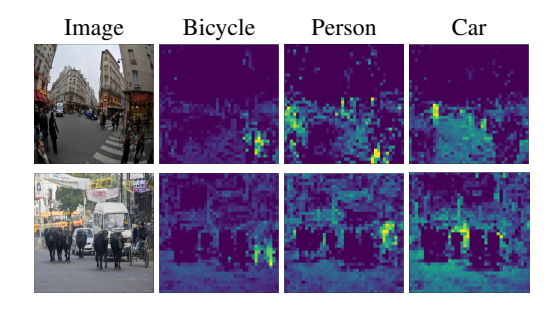


Figure 6. CAM visualization. We show three CAMs correspondence to three particular semantic classes, *i.e.* bicycle, person and car in the same image.

formation from the noisy pseudo label. The performance is further improved as more iterations of the teacher-student bootstrapping are introduced.

Dataset	initial	trained	bootstrapped
COCO-Stuff-27	8.95	13.19	16.19
COCO-Stuff-171	5.05	8.66	11.93
COCO-80	4.23	8.28	12.69

Table 2. Results of bootstrap mechanism.

Loss			mIoU	ACC	
CE	Peer	unc	div	illioc	ACC
✓				10.49	29.72
\checkmark		\checkmark		10.88	31.94
\checkmark		\checkmark	\checkmark	11.34	32.62
	\checkmark			10.54	30.46
	\checkmark	\checkmark		11.24	33.03
	\checkmark		\checkmark	10.96	32.45
	✓	✓	✓	11.93	34.32

Table 3. Results for different losses on COCO-Stuff-171.

The Bootstrapping Loss. We compare different combinations of using the original CE loss, peer loss in Eq. (13), uncertainty loss in Eq. (14), and diversity loss in Eq. (15) in Table 3. Each of the proposed three bootstrapping losses can effectively improve the performance upon the original CE loss, and their combination achieves the best performance.

The Foreground Prior. Experiments of clustering the semantic features without separating the patches with foreground prior will result in the drop of mIoU from 11.93 to 9.52 on COCO-Stuff-171, indicating that the separation of foreground and background patches are helpful to improve the quality of semantic feature clustering.

The Quality of Cropping. An extra experiment is conducted by using ground-truth labels instead of sliding windows to crop the foreground and background objects in a more precise way, which can be regarded as an upper limit of our cropping operation. The mIoU on COCO-Stuff-171 is slightly improved from 11.93 to 12.16. This shows that, even though the sliding window cropping cannot generate precise boxes around semantic objects, it still has exploited sufficient semantic information, leaving not much room to improve compared with the ground-truth cropping.

The Pretrained Encoder. Some baseline methods, *i.e.* PiCIE, use ResNet pretrained on ImageNet in a supervised way as the backbone. For a fair comparison, we conduct two experiments: (1) replace the ResNet-50 backbone of PiCIE with a ResNet-50 pre-trained with DINO on ImageNet; (2) replace the ResNet-50 backbone of PiCIE with a ViT model pre-trained with DINO on ImageNet (the same network as ours). To obtain the input feature maps of FPN used in PiCIE, we extract pixel features every three attention blocks amount 12 layers and resize them to the target size. The modified PiCIE is re-trained on COCO-Stuff-27

Mathod	mIoU	ACC
PiCIE-R50 [10]	5.61	29.79
PiCIE-R50* [10]	2.30	13.50
PiCIE-ViT* [10]	3.02	18.45
TransFGU*	11.93	34.32

Table 4. Results for the effectiveness of pretrained weight. * indicates the model uses the backbone pretrained on DINO.

Image	Prediction	GT	Image	Prediction	GT
	Ne		Flushed VCCC, Belline		(S)
					\$ \$2\$ \$2\$ \$

Figure 7. Failure Cases. left: misclassified; right: missegmented.

and the results are shown in Table 4. The performance of PiCIE with backbones trained in SSL becomes much inferior to its original version. It might be due to the feature learned by SSL containing more fine-grained foreground details, which may distract the bottom-up method to find similar features that belong to the same category. More experiments are included in the supplemental materials, showing the influence of different pre-trained encoders on our method.

4.5. Limitations and Failure Cases

Since our segmentation is based on the high-level semantic representation, similar categories may confuse the classification (The two cases in the left column of Figure 7). Besides that, other challenging cases would also cause failure of our method, *e.g.*, occlusions (top-right in Figure 7), and tiny objects (bottom-right in Figure 7).

5. Conclusion

We propose the first top-down framework for unsupervised semantic segmentation, which shows the importance of high-level semantic information in this task. The semantic prior information is learned from large-scale visual data in a self-supervised manner, and then mapped to the pixel-level feature space. By carefully designing the mapping process and the unsupervised training mechanism, we obtain fine-grained segmentation for both foreground and background. Our design also enables the flexible control of granularity levels of the semantic categories, making it possible to generate semantic segmentation results for various datasets with different requirements. The fully unsupervised manner and the flexibility make our method much more practical in real applications.

Acknowledgements

This work was supported by Alibaba Group through Alibaba Research Intern Program, funds for National Key R&D Program of China(2021YFF0900004), Key R&D Program of Hunan(2022SK2104), leading plan for scientific and technological innovation of high-tech industries of Hunan(2022GK4010), and the National Natural Science Foundation of China (61672222).

References

- [1] Rameen Abdal, Peihao Zhu, Niloy Mitra, and Peter Wonka. Labels4free: Unsupervised segmentation using stylegan. arXiv preprint arXiv:2103.14968, 2021. 3
- [2] Adam Bielski and Paolo Favaro. Emergence of object segmentation in perturbed generative models. In *Proceedings* of the 33rd International Conference on Neural Information Processing Systems, pages 7256–7266, 2019. 3
- [3] Mathilde Caron, Ishan Misra, Julien Mairal, Priya Goyal, Piotr Bojanowski, and Armand Joulin. Unsupervised learning of visual features by contrasting cluster assignments. 2020.
- [4] Mathilde Caron, Hugo Touvron, Ishan Misra, Hervé Jégou, Julien Mairal, Piotr Bojanowski, and Armand Joulin. Emerging properties in self-supervised vision transformers. In Proceedings of the International Conference on Computer Vision (ICCV), 2021. 2, 3, 6, 11
- [5] Hila Chefer, Shir Gur, and Lior Wolf. Transformer interpretability beyond attention visualization. In *Proceedings of the IEEE/CVF Conference on Computer Vision and Pattern Recognition*, pages 782–791, 2021. 4
- [6] Mickaël Chen, Thierry Artières, and Ludovic Denoyer. Unsupervised object segmentation by redrawing. In *Advances in Neural Information Processing Systems 32 (NIPS 2019)*, pages 12705–12716. Curran Associates, Inc., 2019. 3
- [7] Ting Chen, Simon Kornblith, Mohammad Norouzi, and Geoffrey Hinton. A simple framework for contrastive learning of visual representations. In *International Conference on Machine Learning*, pages 1597–1607. PMLR, 2020. 2
- [8] Xinlei Chen, Haoqi Fan, Ross Girshick, and Kaiming He. Improved baselines with momentum contrastive learning. arXiv preprint arXiv:2003.04297, 2020. 2
- [9] Xinlei Chen and Kaiming He. Exploring simple siamese representation learning. In *Proceedings of the IEEE/CVF Conference on Computer Vision and Pattern Recognition*, pages 15750–15758, 2021.
- [10] Jang Hyun Cho, Utkarsh Mall, Kavita Bala, and Bharath Hariharan. Picie: Unsupervised semantic segmentation using invariance and equivariance in clustering. In *Proceedings* of the IEEE/CVF Conference on Computer Vision and Pattern Recognition, pages 16794–16804, 2021. 1, 2, 5, 6, 7, 8,
- [11] Marius Cordts, Mohamed Omran, Sebastian Ramos, Timo Rehfeld, Markus Enzweiler, Rodrigo Benenson, Uwe Franke, Stefan Roth, and Bernt Schiele. The cityscapes dataset for semantic urban scene understanding. In *Proceed*-

- ings of the IEEE conference on computer vision and pattern recognition, pages 3213–3223, 2016. 2
- [12] Alexey Dosovitskiy, Lucas Beyer, Alexander Kolesnikov, Dirk Weissenborn, Xiaohua Zhai, Thomas Unterthiner, Mostafa Dehghani, Matthias Minderer, Georg Heigold, Sylvain Gelly, et al. An image is worth 16x16 words: Transformers for image recognition at scale. arXiv preprint arXiv:2010.11929, 2020. 3
- [13] Mark Everingham, Luc Van Gool, Christopher KI Williams, John Winn, and Andrew Zisserman. The pascal visual object classes (voc) challenge. *International journal of computer* vision, 88(2):303–338, 2010. 2
- [14] Ke Gong, Xiaodan Liang, Dongyu Zhang, Xiaohui Shen, and Liang Lin. Look into person: Self-supervised structuresensitive learning and a new benchmark for human parsing. In Proceedings of the IEEE Conference on Computer Vision and Pattern Recognition, pages 932–940, 2017. 2, 11
- [15] Jean-Bastien Grill, Florian Strub, Florent Altché, Corentin Tallec, Pierre Richemond, Elena Buchatskaya, Carl Doersch, Bernardo Pires, Zhaohan Guo, Mohammad Azar, et al. Bootstrap your own latent: A new approach to self-supervised learning. In *Neural Information Processing Systems*, 2020. 2, 6
- [16] Robert Harb and Patrick Knöbelreiter. Infoseg: Unsupervised semantic image segmentation with mutual information maximization. 2021. 1, 2
- [17] Kaiming He, Haoqi Fan, Yuxin Wu, Saining Xie, and Ross Girshick. Momentum contrast for unsupervised visual representation learning. In *Proceedings of the IEEE/CVF Con*ference on Computer Vision and Pattern Recognition, pages 9729–9738, 2020. 2
- [18] Kaiming He, Georgia Gkioxari, Piotr Dollár, and Ross Girshick. Mask r-cnn. In *Proceedings of the IEEE international conference on computer vision*, pages 2961–2969, 2017. 6
- [19] Jyh-Jing Hwang, Stella X Yu, Jianbo Shi, Maxwell D Collins, Tien-Ju Yang, Xiao Zhang, and Liang-Chieh Chen. Segsort: Segmentation by discriminative sorting of segments. In *Proceedings of the IEEE/CVF International Con*ference on Computer Vision, pages 7334–7344, 2019. 3
- [20] Xu Ji, Joao F Henriques, and Andrea Vedaldi. Invariant information clustering for unsupervised image classification and segmentation. In *Proceedings of the IEEE/CVF International Conference on Computer Vision*, pages 9865–9874, 2019. 1, 2, 5, 6, 7
- [21] Asako Kanezaki. Unsupervised image segmentation by backpropagation. In 2018 IEEE international conference on acoustics, speech and signal processing (ICASSP), pages 1543–1547. IEEE, 2018. 1, 2, 3
- [22] Dahye Kim and Byung-Woo Hong. Unsupervised segmentation incorporating shape prior via generative adversarial networks. In *Proceedings of the IEEE/CVF International Con*ference on Computer Vision, pages 7324–7334, 2021. 3
- [23] Wonjik Kim, Asako Kanezaki, and Masayuki Tanaka. Unsupervised learning of image segmentation based on differentiable feature clustering. *IEEE Transactions on Image Processing*, 29:8055–8068, 2020. 1, 2
- [24] Chunyuan Li, Jianwei Yang, Pengchuan Zhang, Mei Gao, Bin Xiao, Xiyang Dai, Lu Yuan, and Jianfeng Gao. Efficient

- self-supervised vision transformers for representation learning. *arXiv preprint arXiv:2106.09785*, 2021. 2
- [25] Xiaoni Li, Yu Zhou, Yifei Zhang, Aoting Zhang, Wei Wang, Ning Jiang, Haiying Wu, and Weiping Wang. Dense semantic contrast for self-supervised visual representation learning. arXiv preprint arXiv:2109.07756, 2021. 2
- [26] Tsung-Yi Lin, Michael Maire, Serge Belongie, James Hays, Pietro Perona, Deva Ramanan, Piotr Dollár, and C Lawrence Zitnick. Microsoft coco: Common objects in context. In European conference on computer vision, pages 740–755. Springer, 2014. 2, 6
- [27] Yang Liu and Hongyi Guo. Peer loss functions: Learning from noisy labels without knowing noise rates. In *Interna*tional Conference on Machine Learning, pages 6226–6236. PMLR, 2020. 5
- [28] S Ehsan Mirsadeghi, Ali Royat, and Hamid Rezatofighi. Unsupervised image segmentation by mutual information maximization and adversarial regularization. *IEEE Robotics and Automation Letters*, 6(4):6931–6938, 2021. 1, 2, 3
- [29] Yassine Ouali, Céline Hudelot, and Myriam Tami. Autoregressive unsupervised image segmentation. In *European Conference on Computer Vision*, pages 142–158. Springer, 2020. 2
- [30] Pedro O Pinheiro, Amjad Almahairi, Ryan Y Benmalek, Florian Golemo, and Aaron C Courville. Unsupervised learning of dense visual representations. In *NeurIPS*, 2020. 2
- [31] Ramprasaath R Selvaraju, Michael Cogswell, Abhishek Das, Ramakrishna Vedantam, Devi Parikh, and Dhruv Batra. Grad-cam: Visual explanations from deep networks via gradient-based localization. In *Proceedings of the IEEE international conference on computer vision*, pages 618–626, 2017. 2, 4
- [32] Robin Strudel, Ricardo Garcia, Ivan Laptev, and Cordelia Schmid. Segmenter: Transformer for semantic segmentation. In *Proceedings of the IEEE/CVF International Conference on Computer Vision*, 2021. 4, 6
- [33] Wouter Van Gansbeke, Simon Vandenhende, Stamatios Georgoulis, and Luc Van Gool. Unsupervised semantic segmentation by contrasting object mask proposals. In *Interna*tional Conference on Computer Vision, 2021. 1, 3, 6, 7
- [34] Xinlong Wang, Rufeng Zhang, Chunhua Shen, Tao Kong, and Lei Li. Dense contrastive learning for self-supervised visual pre-training. In *Proceedings of the IEEE/CVF Con*ference on Computer Vision and Pattern Recognition, pages 3024–3033, 2021. 2
- [35] Zhaoqing Wang, Qiang Li, Guoxin Zhang, Pengfei Wan, Wen Zheng, Nannan Wang, Mingming Gong, and Tongliang Liu. Exploring set similarity for dense self-supervised representation learning. arXiv preprint arXiv:2107.08712, 2021.
- [36] Zhenda Xie, Yutong Lin, Zheng Zhang, Yue Cao, Stephen Lin, and Han Hu. Propagate yourself: Exploring pixel-level consistency for unsupervised visual representation learning. In Proceedings of the IEEE/CVF Conference on Computer Vision and Pattern Recognition, pages 16684–16693, 2021.

- [37] Jiarui Xu and Xiaolong Wang. Rethinking self-supervised correspondence learning: A video frame-level similarity perspective. *arXiv preprint arXiv:2103.17263*, 2021. 2
- [38] Zhuliang Yao, Yue Cao, Yutong Lin, Ze Liu, Zheng Zhang, and Han Hu. Leveraging batch normalization for vision transformers. In *Proceedings of the IEEE/CVF International Conference on Computer Vision*, pages 413–422, 2021. 2, 11
- [39] Jianming Zhang, Sarah Adel Bargal, Zhe Lin, Jonathan Brandt, Xiaohui Shen, and Stan Sclaroff. Top-down neural attention by excitation backprop. *International Journal of Computer Vision*, 126(10):1084–1102, 2018. 2

Supplementary Material

In this supplementary material, we first present two more ablation studies to reveal the effectiveness of the encoder, decoder, and semantic prior model used in our pipeline. Then we show our re-defined labels for 5 and 16 categories in LIP. Finally, more qualitative results on Cityscapes are presented.

The effectiveness of encoder and decoder. To evaluate the effectiveness of the encoder and decoder used in our top-down pipeline, we conduct three more experiments that gradually replace the encoder and decoder with the ones used in PiCIE [10]. First, we change the encoder from ViT to ResNet-50 followed by an FPN model and keep the decoder as Segmenter. Second, we keep the encoder as ViT and change the decoder from Segmenter to a single layer convolution classifier, which is used in PiCIE, to map the output dimension of the last attention block from d to K. Last, the encoder and decoder are replaced by ResNet-50 and convolution classifier, respectively. In all the settings, the encoders (ViT, ResNet-50) are trained on the ImageNet by DINO, and the decoders (Segmenter, convolution classifier) are randomly initialized. The results are shown in Table 5. As one can see, in all the settings, the performance can be improved from the initial pseudo label (encoder and decoder are all set to 'None'). Moreover, it's important to use fully-transformer architecture in our pipeline due to its robustness to noises.

The effectiveness of the semantic prior model. We conduct two more experiments to reveal the effectiveness of the semantic prior model. The results are shown in Table 6. We first change the semantic prior model from ViT small 8x8 to ViT small 16x16 trained by DINO [4]. The mIoU drop from 11.93 to 9.43. Second, we change the ViT small 16x16 trained by DINO with the one trained by MoCo V3 [38]. The performance drops dramatically to 2.32, which indicates the different manners of self-supervised learning affect the segmentation property of the semantic prior model and results in different performances in our pipeline.

Label definition on LIP under different granularity. We re-defined the LIP [14] under different granularity by merging categories in its original label (19 categories) and generating two new label definitions (16 and 5 categories). The indices projection is shown in Table 7.

decoder	mIoU	ACC
None	5.05	17.33
segmenter	11.93	34.32
segmenter	9.21	26.17
classifier	7.96	24.17
classifier	8.33	25.35
	None segmenter segmenter classifier	None 5.05 segmenter 11.93 segmenter 9.21 classifier 7.96

Table 5. Results for the effectiveness of encoder and decoder.

SSL method	patch size	mIoU	ACC
DINO	8	11.93	34.32
DINO	16	9.43	28.12
MoCoV3	16	2.32	20.94

Table 6. Results for the effectiveness of semantic prior model.

Name	granularity level 19 categories 16 categories 5 categories		
Daakaround	0	0	0
Background	_	Ü	9
Hat	1	1	1
Hair	2	2	1
Glove	3	3	3
Sunglasses	4	4	1
Upper-clothes	5	5	2
Dress	6	6	2
Coat	7	7	2
Socks	8	8	5
Pants	9	9	4
Jumpsuits	10	10	2
Scarf	11	11	2
Skirt	12	12	2
Face	13	13	1
Left-arm	14	14	3
Right-arm	15	14	3
Left-leg	16	15	4
Right-leg	17	15	4
Left-shoe	18	16	5
Right-shoe	19	16	5

Table 7. Label definition on LIP under different granularity.

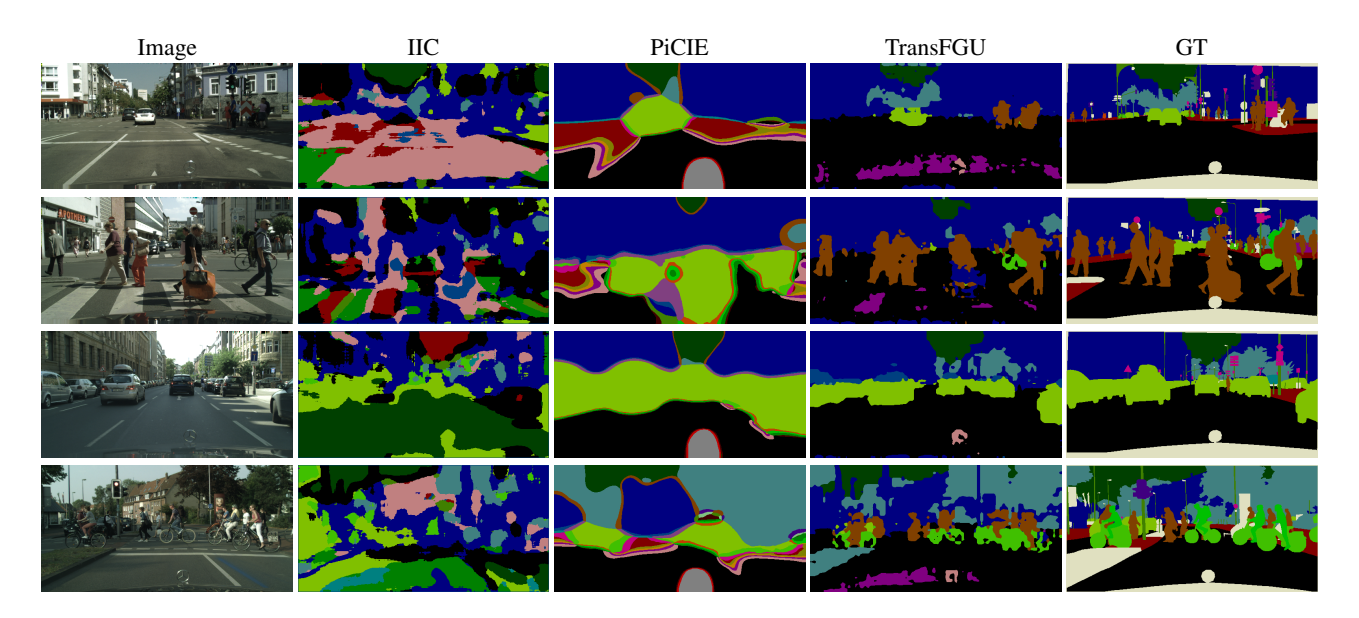


Figure 8. Qualitative comparison on Cityscapes.